

Dynamic Nuclear Polarization of Biocompatible ^{13}C -Enriched Carbonates for *In vivo* pH Imaging

David E. Korenchan^{†‡}, Robert R. Flavell[‡], Celine Baligand[‡], Renuka Sriram[‡], Kiel Neumann[‡], Subramaniam Sukumar[‡], Henry VanBrocklin[‡], Daniel B. Vigneron^{†‡}, David M. Wilson^{‡*}, and John Kurhanewicz^{†‡*}

[†]UC Berkeley-UCSF Graduate Program in Bioengineering, University of California, Berkeley and University of California, San Francisco, California, USA

[‡]Department of Radiology and Biomedical Imaging, University of California, San Francisco, California, USA

Contents

Chemicals	2
Formulation and HP ^{13}C-NMR spectroscopy of sodium ^{13}C-bicarbonate in glycerol at 11.7 T	2
Formulation of glycerol, ethanol, and mannose carbonates	3
HP ^{13}C-NMR spectroscopy at 11.7 T of unenriched GLC, DEPC, and MC following hydrolysis	4
Synthesis of $[1-^{13}\text{C}]$ 1,2-glycerol carbonate	5
HP ^{13}C-NMR spectroscopy of $[1-^{13}\text{C}]$ 1,2-glycerol carbonate at 11.7 T	5
Pulse design and characterization for co-localized excitation of bicarbonate and CO_2 at 14 T	7
HP ^{13}C 2D CSI acquisition and data processing	8
HP phantom imaging for pH quantification at 14 T	8
<i>In vivo</i> HP ^{13}C-NMR pH_e imaging and apparent T_1 measurements in mouse prostate tumors at 14 T	9
Statistical Analyses	11
References	12

Chemicals

1,2-glycerol carbonate (GLC) and diethyl pyrocarbonate (DEPC) were purchased from Fisher Scientific (Pittsburgh, PA). 2,3-O-carbonyl- α -D-mannopyranose (MC, or mannose carbonate) was purchased from Carbosynth (San Diego, CA). Sodium ^{13}C -bicarbonate was purchased from Isotec (Miamisburg, OH), and [$1\text{-}^{13}\text{C}$] 1,2-glycerol carbonate was purchased from either Isotec (Miamisburg, OH) or Cambridge Isotopes Laboratories, Inc. (Tewksbury, MA). The OX063 and GE trityl radicals were purchased from GE Healthcare (Menlo Park, CA). Other chemicals and solvents were purchased from Aldrich (St. Louis, MO).

Formulation and HP ^{13}C -NMR spectroscopy of sodium ^{13}C -bicarbonate in glycerol at 11.7 T

Sodium ^{13}C -bicarbonate in glycerol was formulated for hyperpolarization as previously described.¹ 63 mg of the formulation were polarized at 94.052 GHz and 1.40 K for 25 minutes using a HyperSense DNP polarizer (Oxford Instruments, Abingdon, UK). The sample was then dissolved with 3.5 mL of a 0.3 mM EDTA solution, transferred to a capped 5 mm NMR tube, and placed inside a 37 °C temperature-regulated 500 MHz Varian INOVA spectrometer (Agilent Technologies, Palo Alto, CA) equipped with a 5 mm triple-tuned, direct-detect, triple-axis gradient-equipped broadband probe (Agilent Technologies, Palo Alto, CA). The resulting pH of the dissolution was about 9 (pH strip). Dynamic HP ^{13}C NMR spectra were immediately acquired (TR = 3 s, 30° hard pulses, spectral window -18.9 to 219.9 ppm, 60k FID points, 50 timepoints), and a series of 90° hard pulses was then applied to destroy the remaining HP magnetization. A ^{13}C NMR spectrum was acquired afterward to measure the magnetization at thermal equilibrium (TR = 10 s, 52.7° hard pulses, same spectral width/resolution, 1024 averages). The data were apodized with a 2 Hz line broadening, Fourier transformed, phased, and referenced using ACD/NMR Processor (ACD/Labs, Toronto, Ontario, Canada). Figure S1 displays the results. Notice that the two labeled contaminant peaks appear in the HP spectrum but barely appear above the noise in the thermal spectrum acquired over the subsequent 3.5 hours.

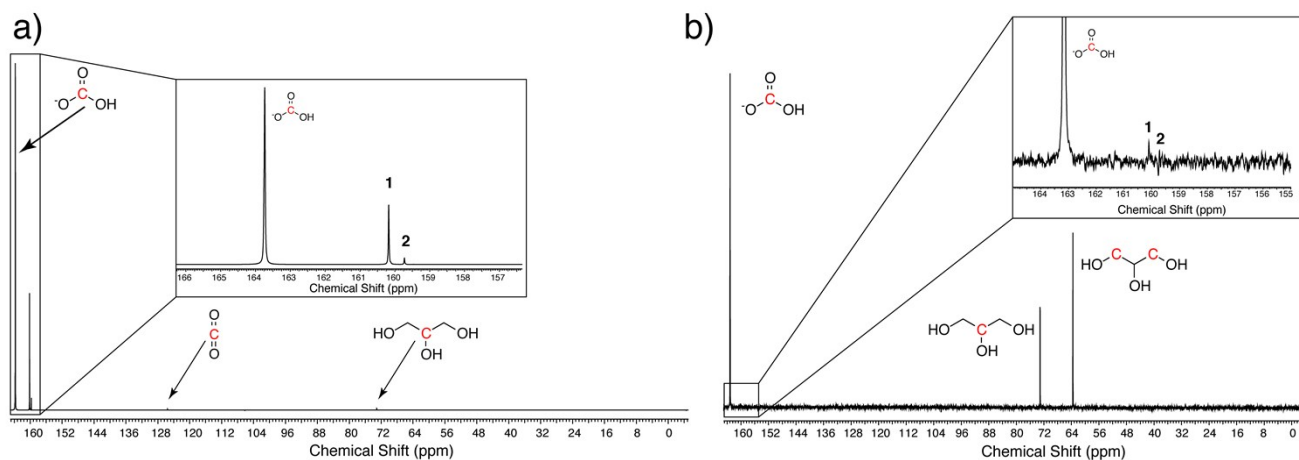


Figure S1: (a) HP ^{13}C NMR spectrum at 11.7 T of ^{13}C -bicarbonate in glycerol dissolved in water + 0.3 mM EDTA. The bicarbonate and contaminant peaks shifted upfield over the course of the HP experiment. Final ppm values: bicarbonate 163.2 ppm; contaminant peak 1 160.1 ppm; contaminant peak 2 159.7 ppm; CO_2 125.5 ppm; C2 glycerol 73.1 ppm (referenced value), C1/C3 glycerol 63.5 ppm. (b) ^{13}C NMR spectrum at 11.7 T of the same dissolution after the magnetization returned to thermal equilibrium (1024 transients averaged together). Final ppm values: bicarbonate 163.2 ppm; contaminant peak 1 160.1 ppm; contaminant peak 2 159.7 ppm; C2 glycerol 73.1 ppm (reference peak); C1/C3 glycerol 63.6 ppm.

Formulation of glycerol, ethanol, and mannose carbonates

Each compound in the study was formulated at the maximum concentration that formed a glassy state upon immediate immersion in liquid nitrogen. Formulation glassing was determined by visual inspection; if the flash-frozen formulation without radical added was transparent, then it was determined to be in a glassy state. Only the 1,2-glycerol carbonate (GLC) was formulated with the ^{13}C -enriched compound.

Glycerol carbonate: 3.1 mg of OX63 trityl radical were added to 207.4 mg (147 μL) of 1,2-glycerol carbonate, to a final concentration of 15 mM. The mixture was sonicated for 5 minutes at room temperature. The same recipe was used for both ^{13}C -enriched and unenriched compound.

Diethyl pyrocarbonate: 3.1 mg of GE trityl radical were dissolved in 14.7 μL dimethyl sulfoxide (DMSO) prior to addition of 103.3 μL of DEPC. The radical concentration was about 15 mM. The mixture was vortexed and sonicated for 2 minutes at room temperature.

Mannose carbonate: 206.6 mg of 2,3-O-carbonyl- α -D-mannopyranose were dissolved in 51.7 μL of water using a combination of vortexing, centrifugation, and sonication. To this solution, 5.2 mg of OX063 trityl radical were added to a final concentration of about 15 mM and dissolved using a similar technique.

HP ^{13}C -NMR spectroscopy at 11.7 T of unenriched GLC, DEPC, and MC following hydrolysis

457 μmol of each formulated compound were placed in a sample cup along with 2 μL of a ~ 6 M urea HP prep and polarized at 94.060 GHz at a temperature of 1.3-1.4 K for 1 hour using a HyperSense DNP polarizer (Oxford Instruments, Abingdon, UK). The sample was then dissolved using 3.5 mL of 270 mM NaOH and 0.3 mM EDTA and ejected into a glass flask that was preheated for ~ 1 minute using a dual-temperature heat gun set to low (Milwaukee Tool, Brookfield, WI). The solution was swirled and heated for 5 seconds in the flask, then subsequently placed in a water bath to cool. 700-750 μL of 750 mM HCl were added to the flask to obtain an approximately neutral pH and swirled to mix. The solution was then transferred to a capped 5 mm NMR tube, inserted into a pre-tuned, pre-shimmed, 37 $^{\circ}\text{C}$ temperature-regulated 500 MHz Varian INOVA spectrometer (Agilent Technologies, Palo Alto, CA), and ^{13}C NMR spectra were acquired using a 5 mm triple-tuned, direct-detect, triple-axis gradient-equipped broadband probe (Agilent Technologies, Palo Alto, CA). The time between the sample leaving the polarizer and the start of acquisition was 31-37 seconds. A series of hyperpolarized spectra was then acquired (TR = 3 s, 20° hard pulse, spectral window 58.7 to 217.8 ppm, 40k FID points, 25 timepoints). For processing, the data were 2 Hz line-broadened, Fourier transformed, phased, referenced, and integrated using VnmrJ 3.2A software (Agilent Technologies, Palo Alto, CA). The % $\text{HCO}_3^- + \text{CO}_2$ for each carbonate (Table 1) was calculated from the first timepoint as the ratio of the total integrated area of the bicarbonate and CO_2 peaks over the total integrated area of all carbonyl- ^{13}C peaks, not including peaks from hydrolysis products (ie. ethanol, glycerol, mannose).

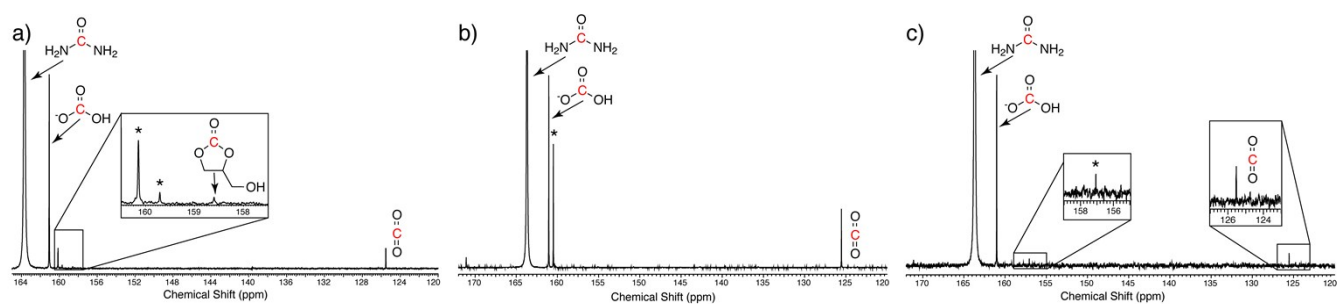


Figure S2: Representative HP spectra of each compound evaluated in the study immediately following hydrolysis. Each compound was copolarized with 2 μL of ^{13}C -urea (referenced to 163.7 ppm in each spectrum). HP ^{13}C -bicarbonate and $^{13}\text{CO}_2$ peaks appeared at 161.1 ppm and 125.5 ppm, respectively. Unidentified hydrolysis product peaks are indicated with an asterisk (*) in each spectrum. Other peaks not within the displayed spectral window but pertaining to known reaction byproducts (ethanol, glycerol) were also seen. (a) 1,2-glycerol carbonate (GLC).

* at 160.1 and 159.7 ppm, GLC at 158.6 ppm. (b) diethyl pyrocarbonate (DEPC). * at 160.5 ppm. (c) 2,3-O-carbonyl- α -D-mannopyranose (MC). * at 157.1 ppm.

Synthesis of [1- 13 C] 1,2-glycerol carbonate

Glycerol (90 mg, 1 mmol) was added to a 25 mL round bottom flask with a magnetic stir bar. Carbonyl- 13 C dimethyl carbonate (200 mg, 2.2 mmol) was then added to the stirring reaction mixture, followed by potassium carbonate (3 mg, 0.02 mmol) and magnesium oxide (3 mg, 0.01 mmol). The reaction mixture was heated at 80 °C for 3 hours, then allowed to cool to room temperature. The mixture was diluted with 20 mL of hexanes and filtered by gravity. The filtered solid was washed with an additional 10 mL aliquot of hexanes. The filtrate fractions were combined and the solvent was removed by rotary evaporation at 40 °C. The flask was then placed under dynamic vacuum for 15 hours, which left a colorless, viscous oil. NMR confirmed the oil to be pure [1- 13 C] 1,2-glycerol carbonate (91 mg, 78% yield). The 1 H chemical shifts and multiplicities corresponded similarly to previous literature.² High-resolution mass spectrometry was also performed on this sample using a microTOF instrument by the Notre Dame mass spectrometry facility (Notre Dame, IN). HR-MS – m/z (microTOF) $C_3^{13}CH_6NaO_4$ ($M+Na^+$) found 142.0183, calculated 142.0192.

HP 13 C-NMR spectroscopy of [1- 13 C] 1,2-glycerol carbonate at 11.7 T

With hydrolysis: 54 mg of [1- 13 C] GLC plus 15 mM OX063 trityl radical were polarized in a HyperSense polarizer at 94.070 GHz, which was determined to be the optimal microwave frequency via a microwave sweep. The buildup in signal was monitored every 300 s via a solid-state NMR spectrometer inside the polarizer, and the points were fit to an exponential buildup curve. The average time constant of the fitted curve was 3170 ± 510 s ($n = 7$). The same post-dissolution procedure was used as for the unlabeled compound, except that the solution was heated for 10 s instead of 5 s (acquisition: TR = 3 s, 5° hard pulse, spectral window 58.7 to 217.8 ppm, 40k FID points, 50 timepoints). The 5 mm NMR tube was capped immediately after adding ~1 mL of HP solution to reduce loss of $^{13}CO_2$. The pH of the solution was measured shortly after dissolution with a conventional pH electrode (Ion 500 series, Oakton Instruments, Vernon Hills, IL). Peak areas from the hyperpolarized spectra were flip angle-corrected and fit to a decaying exponential to approximate T_1 values. The polarization was determined with reference to a spectrum at thermal equilibrium (TR = 5 * [measured T_1], 90° hard pulse, same spectral window/resolution, 4 transients), accounting for differences in flip angle and the transfer time between the

polarizer and spectrometer. Bicarbonate and CO₂ concentration measurements were measured from the thermal equilibrium spectrum by constructing a standard curve using 4 known concentrations of [1-¹³C] glycine in deionized water (data not shown). The glycine spectra and the bicarbonate-CO₂ spectra included an electronic reference signal (ERETIC),³ which showed the same intensity in all spectra and was therefore used to measure concentrations. The pulse widths of the 90° hard pulses used were calibrated for each sample from the 360° zero-crossing.

The extent of completion of hydrolysis was also evaluated using less NaOH (1 equivalent and 1.5 equivalents) in the dissolution. For these experiments, the same post-dissolution procedure as described above was used except that the HP sample was dissolved in either 136 mM (1 eq) or 204 mM (1.5 eq) NaOH + 0.3 mM EDTA. In these cases, the percentage of HP bicarbonate + CO₂ signal of the total was 34.2% and 71.6%, respectively (n = 1 each).

Without hydrolysis: The same experimental procedures were used as in the case with hydrolysis, except for the following. After polarization, 100 mM phosphate buffer at pH 7.8 plus 0.3 mM EDTA was used for dissolution, and no heating or neutralization took place. The transfer time was similar to the unlabeled compound studies for both cases with and without hydrolysis. The T₁ and polarization values were calculated as for the case with hydrolysis.

Table S1: Summary of HP ¹³C-GLC results

With Hydrolysis (n = 3)					
HP HCO ₃ ⁻ T ₁ (s)	HP CO ₂ T ₁ (s)	% Polarization ^a	% HCO ₃ ⁻ +CO ₂ signal ^b	[HCO ₃ ⁻ +CO ₂] (mM) ^c	Expected [HCO ₃ ⁻ +CO ₂] (mM) ^d
33.9 ± 3.9	32.8 ± 3.9	16.4 ± 1.3 (5.2 ± 0.9)	97.3 ± 0.5	75.1 ± 1.4	108.7 ± 2.5

Without Hydrolysis (n = 4)	
HP GLC T ₁ (s)	% Polarization ^a
63.7 ± 5.7	18.1 ± 2.4 (10.8 ± 2.1)

^a Back-calculated to the time of dissolution using the average T₁ value measured in the HP experiment (without back-calculation in parentheses)

^b Calculated from first HP spectrum as HCO₃⁻ + CO₂ peak area over total

^c n = 2 samples

^d Calculated from prep weight and final volume of solution

Pulse design and characterization for co-localized excitation of bicarbonate and CO₂ at 14 T

The ¹³C chemical shifts of bicarbonate and CO₂ are separated by 35.5 ppm, which translates to 5325 Hz at 14 T. Depending on the slice-select gradient strength, this could translate to a large spatial separation between bicarbonate and CO₂ excited slices with a single-band pulse and therefore an inaccurate measurement of pH for a given slice. Therefore, excitation pulses were designed to excite both bicarbonate and CO₂ in a single slice. Each designed pulse was the sum of two phase-modulated Gaussian pulses, resulting in two frequency bands (FWHM = 1500 Hz each) separated by 5325 Hz. These pulses excited both resonances in the center of the coil, provided the transmitter was set in the middle of the two resonances. The excitation slice gradient was kept sufficiently low (< 1.75 G/cm, or a minimum slice thickness of 8 mm for this pulse) such that excitation bands other than those in the center were outside the sensitive volume of the coil. Two pulses were designed: one with equal flip angles on bicarbonate and CO₂ (dual-band 1:1 pulse) and one where the flip angle on CO₂ was 9 times that on bicarbonate (dual-band 1:9 pulse). Both pulses were designed using MATLAB programming language (MathWorks, Natick, MA). Figure S3 shows the results of pulse validation experiments on a ¹H water phantom. In addition, we verified with a ¹³C-lactate phantom extending past the edges of the coil that pulsing with the transmitter set 2662.5 Hz upfield or downfield of the lactate resonance resulted in a single excited slice in the center of the coil (data not shown).

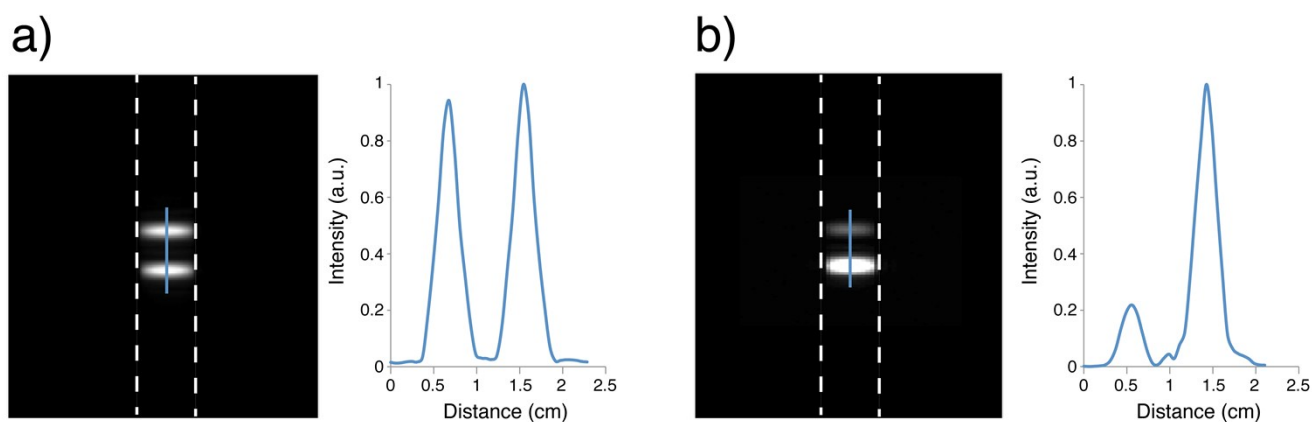


Figure S3: Two-band Gaussian experimental pulse profiles with line plots on a ¹H water phantom, edges defined by dashed lines. (a) Symmetric excitation bands. (b) Upfield excitation band has a 9-fold higher flip angle than the downfield excitation band.

HP ¹³C 2D CSI acquisition and data processing

All phantom and *in vivo* images were acquired on a vertical-bore 14 T Varian NMR imaging system (150 MHz ¹³C, Varian Instruments) equipped with a dual-tuned ¹H/¹³C quadrature coil (m2m Imaging, Cleveland, OH). The pulse sequence was a ¹³C 2D CSI sequence (8 x 8 x 256 matrix size, centric encoding, FOV = 32 x 32 mm, 8013 Hz spectral width, TR = 34 ms, total imaging time ~2 s). One of the two dual-band pulses previously described was used for slice excitation, with the transmitter frequency set in the middle between bicarbonate and CO₂. The ¹³C transmitter frequency was calculated from the measured ¹H offset of the water resonance. The system was tuned and shimmed prior to HP imaging. After the HP ¹³C acquisition, a T₂-weighted ¹H spin-echo axial image was taken for co-registration with the ¹³C data.

The HP data were 10 Hz-apodized spectrally, Fourier-transformed, and visualized using an open-source software, SIVIC (Sourceforge.net). Integrals of the bicarbonate and CO₂ peaks from magnitude spectra were used for analysis. Spectra with a bicarbonate or CO₂ SNR ≤ 3 were excluded from analysis.

HP phantom imaging for pH quantification at 14 T

54 mg of [1-¹³C] GLC were polarized, dissolved, and hydrolyzed as described previously. 0.4-0.5 mL of HP solution were added to each of three 10-mm NMR tubes filled with 3.4-3.6 mL of 100 mM phosphate buffer at three different pH values between 6.3 and 7.6 and kept previously at 37 °C. Just before the dissolution, 18 U/mL of carbonic anhydrase II (CAII, Sigma, St. Louis, MO) were added to each tube. The tubes were briefly vortexed to mix and inserted into the imaging system, which was kept at 37 °C using heated air. The temperature inside the system was calibrated prior via ¹H spectroscopy on ethylene glycol. Two ¹³C 2D CSI sequences were performed, each using a different excitation pulse: first with the [2.78°, 25°] dual-band 1:9 pulse, with the higher flip angle on CO₂, and then with the [10°, 10°] dual-band 1:1 pulse. There was a 5 s delay between acquisitions. For both imaging protocols, the slice thickness was 10 mm. The transfer time between the polarizer and the magnet was ~50 seconds. After imaging, the pH of each tube in the phantom was measured at 37 °C outside the magnet using a conventional pH electrode (Ion 500 series, Oakton Instruments, Vernon Hills, IL) to compare with the pH measured via spectroscopy. Figure S4 displays the phantom ¹H image and overlaid HP ¹³C spectra for both flip

angle schemes (same data as Figure 2c, but with full FOV displayed). The pH map in Figure S4 is displayed only for voxels with $\text{SNR} \geq 5$.

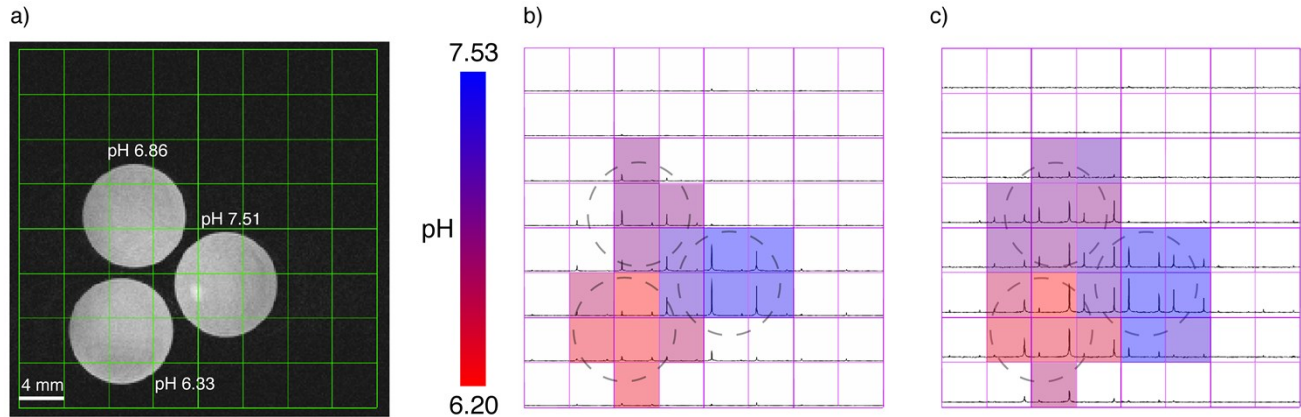


Figure S4: (a) Axial T₂-weighted ¹H image of the pH imaging phantom. (b) HP ¹³C 2D CSI data using the [10°, 10°] dual-band 1:1 pulse. (c) HP ¹³C 2D CSI data using the [2.78°, 25°] dual-band 1:9 pulse. Tube boundaries are indicated with dashed lines on the two spectroscopic data sets. Note that the data in (c) were acquired in the same experiment just before those in (b).

***In vivo* HP ¹³C-NMR pH_e imaging and apparent T₁ measurements in mouse prostate tumors at 14 T**

All animal experiments were performed under a protocol approved by the UCSF Institutional Animal Care and Utilization Committee. A transgenic adenocarcinoma of the mouse prostate (TRAMP) model mouse was anesthetized using a mixture of oxygen and isoflurane, and a catheter was inserted into the tail vein. The mouse was then secured in an MR-compatible holder with a 37 °C water pad and inserted into the vertical bore of the imaging system. 54 mg of [1-¹³C] GLC were polarized, dissolved, and hydrolyzed as previously described, and 350-400 uL of HP dissolution were injected into the mouse over 12 seconds. The total injected dose was ~27 μmol of ¹³C-GLC, or 3.2 mg (~100 mg/kg).

pH_e imaging: For imaging, a 2D CSI sequence was initiated 1 s after the end of injection, with experimental parameters as described above. After zero-filling to 16 x 16 x 256 and processing the data as mentioned above, the average pH_e values within the tumor (n = 13 voxels) and vasculature (n = 8 voxels) were calculated. For the tumor, the bottom row of voxels was excluded from analysis due to these voxels encompassing both tumor and normal tissue. Figure S5 displays the anatomical ¹H image and overlaid *in vivo* HP ¹³C spectra (same data as Figure 3, but with full FOV displayed).

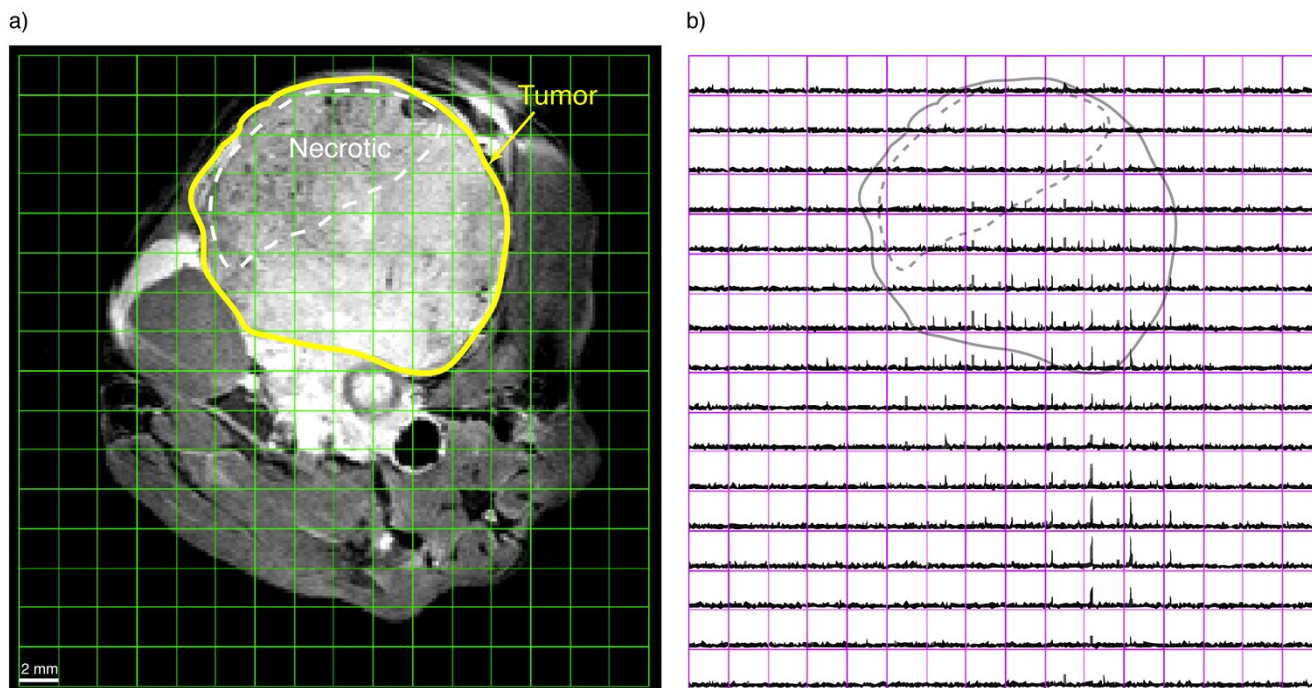


Figure S5: (a) Axial T₂-weighted ¹H image of the TRAMP mouse, including tumor and necrotic regions outlined in yellow and white, respectively. (b) HP ¹³C 2D CSI data, with tumor and necrotic regions outlined in solid and dashed lines, respectively.

Apparent T₁ measurements: Series of dynamic ¹³C NMR spectra (TR = 3 s, spectral window 20.1 kHz, 40k FID points) were acquired utilizing the [30°, 30°] dual-band 1:1 pulse centered on the tumor in the middle of the coil. Acquisition was started immediately after the start of injection. To measure the apparent T₁, the phased spectral peak areas were determined using VnmrJ 3.2A software (Agilent Technologies, Palo Alto, CA) and fit to an exponential curve without flip angle correction within MATLAB (MathWorks, Natick, MA), starting at the timepoint with the maximum signal and including 6 timepoints. All spectral peaks used for fitting had a SNR ≥ 3. Figure S6 displays a representative set of dynamic ¹³C NMR spectra acquired *in vivo* with HP ¹³C-GLC.

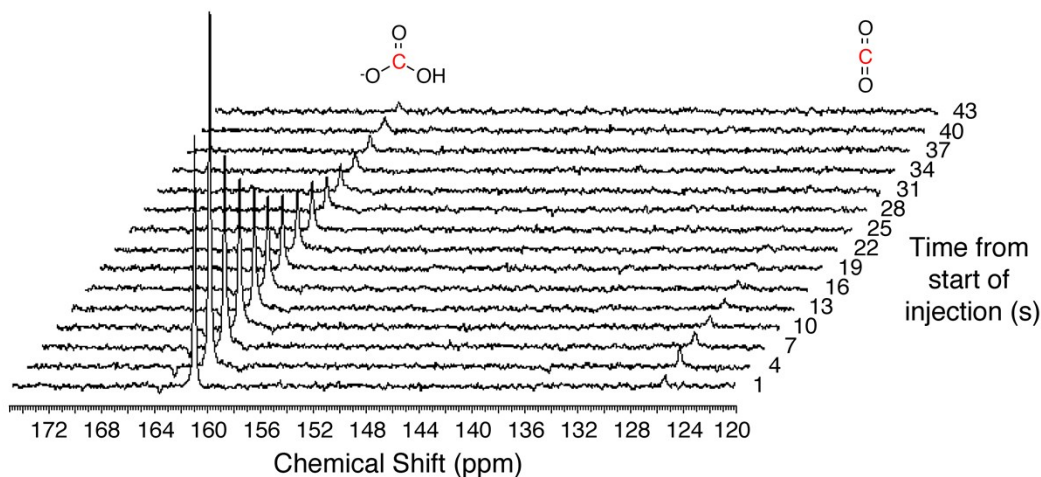


Figure S6: Representative HP ^{13}C GLC dynamic spectra acquired from a slice in a TRAMP murine model.

Literature comparison of solution-state and *in vivo* T_1 values for HP bicarbonate and CO_2

Table S2 summarizes the apparent T_1 relaxation time constants for bicarbonate and CO_2 measured across several studies, including this one, both in solution and *in vivo*. Literature results agree that bicarbonate and CO_2 do not have a statistically significant difference in T_1 , either in solution¹ or *in vivo*.⁴ This is attributed to the rapid interconversion rate between bicarbonate and CO_2 .⁴ Although the apparent *in vivo* T_1 values measured in this study are comparable to those previously reported, we measured lower solution-state T_1 values than Wilson et al. This subtle variation may be due to slight variations in temperature, pH, and measurement technique.

Table S2: Literature comparison of bicarbonate and CO_2 T_1 values

Literature Comparison of Bicarbonate and CO_2 T_1 Values				
HP HCO_3^- T_1 (s)	HP CO_2 T_1 (s)	Measurement Type	Field Strength (T)	Reference
43.3 ± 1.2	44.7 ± 0.6	Solution-state	11.7	(1)
33.9 ± 3.9	32.8 ± 3.9	Solution-state	11.7	This study
10.1 ± 2.9	9.8 ± 2.5	<i>In vivo</i> , implanted mouse tumor	9.4	(4)
14.4 ± 2.4	14.3 ± 3.0	<i>In vivo</i> , transgenic mouse tumor	14	This study

Statistical Analyses

All statistical analyses were performed using R, an open-source software (R-project.org). Statistical significance was determined using a two-tailed student's t-test with unequal variances and sample sizes. A p-value of $p < 0.05$ was considered to be statistically significant.

References

- (1) Wilson, D. M.; Keshari, K. R.; Larson, P. E. Z.; Chen, A. P.; Hu, S.; Crieckinge, M. V.; Bok, R.; Nelson, S. J.; Macdonald, J. M.; Vigneron, D. B.; Kurhanewicz, J. *Journal of Magnetic Resonance*. July 2010, pp 141–147.
- (2) Rokicki, G.; Rakoczy, P.; Parzuchowski, P.; Sobiecki, M. *Green Chemistry*. 2005, p 529.
- (3) Barantin, L.; Pape, A. L.; Akoka, S. *Magnetic Resonance in Medicine*. Wiley Online Library 1997, pp 179–182.
- (4) Gallagher, F. A.; Kettunen, M. I.; Day, S. E.; Hu, D.-E.; Ardenkjaer-Larsen, J. H.; Zandt, R. I. T.; Jensen, P. R.; Karlsson, M.; Golman, K.; Lerche, M. H.; Brindle, K. M. *Nature*. May 28, 2008, pp 940–943.